

Fracture Behavior of Dynamically Vulcanized Thermoplastic Elastomers

ALAN J. LESSER, NATHAN A. JONES

Polymer Science and Engineering Department, Silvio O. Conte Research Center, University of Massachusetts, Amherst, Massachusetts 01003

Received 21 December 1998; accepted 22 June 1999

ABSTRACT: The energetics and micromechanisms of fracture in model dynamically vulcanized thermoplastic elastomers have been studied. Their fracture toughness values have been quantified under mode I loading conditions using both the critical J-integral approach and an essential work-of-fracture method. Additional studies evaluating the effect of specimen geometry are reported. For these studies it was found that center-notched and double edge-notched test geometries were equivalent under J-integral test conditions. The effect of elastomer composition was also studied with regard to fracture resistance. Increasing the weight percentage of both elastomer and processing oil caused a considerable decrease in both the material's resistance to both fracture initiation and fracture propagation. Increasing the molecular weight of the thermoplastic phase caused a smaller reduction in fracture resistance. The phase morphology of one model compound, TPE6114, consists of an isotactic polypropylene-rich matrix containing discrete elastomer-rich domains of a diameter of 1–3 μm . A process zone was associated with fracture in this material. The process zone consists of an array of voids and crazes that were 10–30 μm in diameter, an order of magnitude larger than the elastomer-rich domains. These were characterized by scanning electron microscopy (SEM) and optical microscopy. The crazes were found to grow at an angle oblique to the overall crack growth direction. Ruthenium stained SEM samples showed that these crazes and voids occur in both the polypropylene and elastomer domains, and that at least some of the craze fibrils are composed of the elastomeric phase. © 2000 John Wiley & Sons, Inc. *J Appl Polym Sci* 76: 763–770, 2000

Key words: thermoplastic elastomer; fracture toughness; process zone; J-integral, method of essential work

INTRODUCTION

Over the recent years, dynamically vulcanized ethylene propylene diene monomer rubber (EPDM)–polypropylene ThermoPlastic Elastomers (EPTPEs) have gained significant interest by the polymer community due to their complex mor-

phologies and unique properties. Excellent discussions showing the range of morphologies and basic properties that can be obtained with EPTPE alloys have been reported by others.^{1,2}

The purpose of this communication is to describe the energetics and micromechanisms of fracture in model EPTPEs subjected to Mode I loading conditions on relatively thin specimens. The difficulties inherent in conducting these fracture studies are twofold. First, the large reversible deformation that occurs in the vicinity of the crack, due to the elastomeric nature of the material, significantly alters the stress singularity

Correspondence to: A. J. Lesser.
Contract grant sponsors: Advanced Elastomer Systems and Exxon Chemical Company.

Journal of Applied Polymer Science, Vol. 76, 763–770 (2000)
© 2000 John Wiley & Sons, Inc.

during loading. Second, the large irreversible deformation that occurs as a consequence of both the material behavior and specimen thickness negates the assumption of small-scale yielding and requires that nonlinear fracture studies be conducted on these materials.

Early studies have been conducted by Thomas to develop a characteristic energy criterion for thin vulcanized elastomers.^{3,4} In their work, Thomas and coworkers proposed a Griffith-type criterion as well as three different test geometries for this class of crosslinked materials. However, it is well established that a Griffith-type criterion cannot be applied to materials that dissipate significant energy during the fracture process, which is typical for thermoplastics. Hence, alternative methods must be sought.

For ductile materials, two approaches have been adopted to characterize their fracture behavior. The most widely used parameter for characterizing fracture in ductile materials is the *J*-integral approach proposed by Rice.⁵ Traditionally, fracture characterized by this method requires that the specimen must meet certain size constraints to generate a plane-strain condition.⁶ A second approach used to characterize the fracture of ductile materials is referred to as the Essential Work.⁷ In this method, the total work of fracture is considered to be made of two components; one associated with the initiation of the instability (essential part), and the other associated with the plastic deformation in the plane-stress condition (inessential part). More recent studies by Paton and Hashemi studied the equivalence of both of these approaches to characterize the plane-stress fracture behavior.⁸

This article investigates the use of both *J*-integral and essential work methods to characterize the fracture behavior of these materials under Mode I loading conditions. The single-specimen *J*-integral approach is considered for the comparison because this method, if validated, reduces the sample volume requirements necessary for screening studies. The effect of specimen geometry is also investigated with regard to the *J*-integral tests.

Finally, the effect of elastomer morphology and composition are investigated. The *J*-integral fracture resistance is measured for a range of elastomer compositions. We also investigate the damage that occurs in the process zone of the crack tip of one of the compositions, and discuss its scale and form with relation to the morphology of the EPTPEs.

Table I Weight Percentage Composition of the Various Thermoplastic Elastomers Discussed in this Article

Formulation	iPP Content	Elastomer Content	Processing Oil Content	MFR of iPP
TPE6114	50%	25%	25%	20
TPE6112	50%	25%	25%	0.7
TPE6101	20%	40%	40%	20

MFR, melt flow rate.

EXPERIMENTAL

Materials

Three formulations designated as TPE6101, TPE6112, and TPE6114 were provided to us by Advanced Elastomer Systems, L. P. Details of these model EPTPE alloys are given in Table I. Samples were compression molded into plaques 3-mm thick, 200-mm long and 105-mm wide in a hot press. The polymer was melted at 200°C, pressed to 3.5 MPa, and cooled to room temperature by flowing cold water through pipes in the hot press while maintaining the pressure at 3.5 MPa.

J-Integral Tests

Either center-notched or double edge-notched test specimens were fabricated for the *J*-integral tests. The center-notched specimens were fabricated from the compression-molded plaques by cutting a 38-mm notch parallel to the plaques length using a new razor blade. Similarly, the double edge-notched test specimens were fabricated by cutting two 19-mm notches on opposing sides of the plaque parallel to its length. Each specimen was then clamped along the entire specimen length using specially designed clamping fixtures. After clamping the specimen, the gauge width reduced to 64 mm.

The fracture tests were conducted on an Instron Model 1123. The sample was cyclically loaded between its initial position and a maximum extension, which was increased at a rate of 2 mm per cycle. All tests were conducted at a crosshead speed of 25.5 mm/min and the crack lengths were measured optically with a Zeiss stereomicroscope. All crack lengths were measured at the minimum load of each cycle. A typical load–

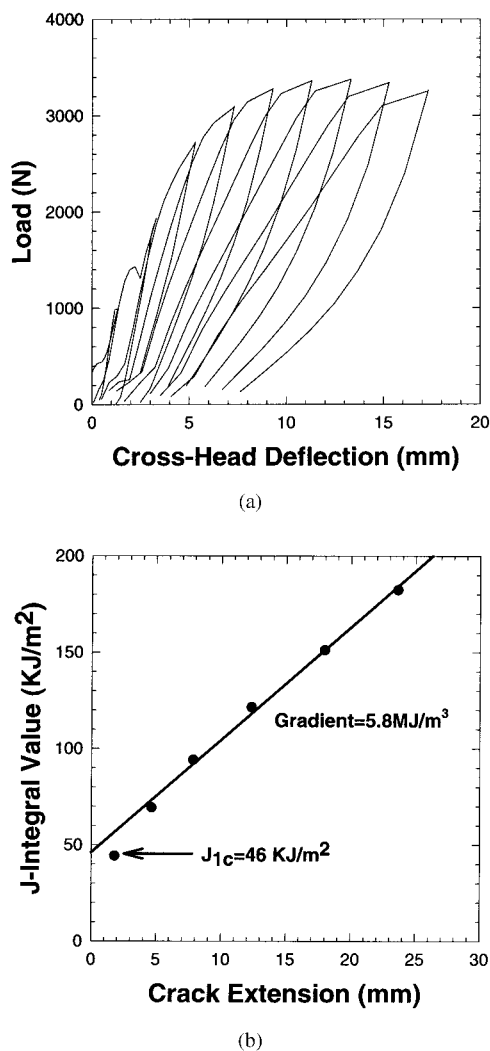


Figure 1 (A) Load deflection curve for the TPE6114 J-integral center notched test. (B) Plot of Energy Release Rate (J) vs. crack extension for TPE6114 fabricated into a center-notched test sample. J_{1c} was calculated from the intercept of the extrapolated data with the J-integral value axis.

displacement curve for a center-notched test specimen is presented in Figure 1(a).

The fracture energies were calculated using a single-specimen test method close to that described in the ASTM E813.⁴ The nonlinear energy release rate, J , was calculated by

$$J_i = \frac{\nu U_i}{BL} \quad (1)$$

where U_i is the energy consumed in the propagation of the crack (area under the load–deflection

curve), B is the specimen thickness, and L is the ligament length ($W - a$, where W is the plaque length and a is the total crack length). η is a dimensionless constant reflecting the geometry of the specimen. For both the center-notched and double-edge notched fracture specimens η equals 1.

Method of Essential Work

Center-notched samples were prepared in the same manner as for the J-integral tests except that the crack lengths were varied between 45 and 164 mm (corresponding to total ligament lengths of between 153 and 34 mm). As before, fracture tests were conducted on an Instron Model 1123. Unlike the J-Integral tests, these samples were monotonically loaded to failure at a crosshead speed of 25.5 mm/min. The crosshead position and load were recorded digitally. From this data the total work of fracture was calculated. The total work of fracture was then decomposed into essential and inessential components as described by eq. (2).⁵

$$w_f = w_e + \beta w_i L \quad (2)$$

In eq. (2) the total work of fracture w_f is described in terms of w_e is the essential work of fracture (deemed to be a material property in this theory), β is the shape factor, w_i is the inessential work of fracture, and L is the ligament length. Tests were conducted on center-notched specimens where the total work of fracture was measured from a series of different specimens containing a range of ligament lengths. The essential work was then calculated by extrapolating the measured values of specific work to a zero ligament length.

RESULTS AND DISCUSSION

Effect of Test Method

A series of experiments were conducted to evaluate the equivalence between various methods of evaluating the fracture energy and isolate any geometric effects. Center-notched specimens of the TPE6114 elastomer were tested in accordance with a single specimen J-integral approach and by the essential work of the fracture method, which is a multiple specimen approach. The results from the center-notched J-integral tests are

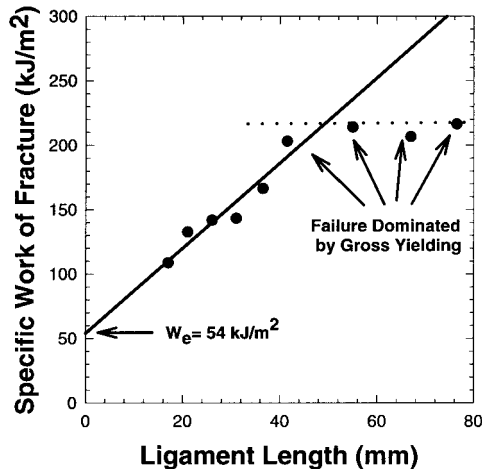


Figure 2 Work of fracture for TPE6114 samples with a range of ligament lengths. The essential work of fracture is given by the extrapolated work of fracture for zero ligament length. Note that for ligament lengths longer than 80 mm the work of fracture becomes independent of the ligament length.

shown in Figure 1, with Figure 1(a) showing the load deflection curves for nine cycles of crack extension, and Figure 1(b) showing the corresponding values of fracture energy. Note in Figure 1(b) that the critical fracture energy measured on the center-notched specimen of TPE6114 was 46 kJ/M^2 , with a slope in the $J - \Delta a$ curve of 5.8 MJ/M^3 . This indicates that this formulation is relatively tough for an elastomeric material and that after fracture (tearing) initiates the process is stable over the entire range of observed extensions. It should be noted that no offset was used in this estimate because the crack extensions were measured optically and no blunting line is necessary.

The results from the essential work experiments for elastomer formulation TPE6114 are summarized in Figure 2. Inspection of the results in Figure 2 indicates that two regimes are present. One regime indicates that the specific work of fracture is independent of ligament length. Note that this regime occurs at relatively long ligament lengths, which indicates that the failure of the elastomer is dominated by gross yielding of the material, and is not significantly altered by the presence of the flaw. In the second regime (i.e., at shorter ligament lengths) the flaw does affect the total work of fracture. In this regime, the data are extrapolated to a zero ligament length to isolate the essential work of fracture. Results from this analysis indicate an essential

work of fracture for this material is 54 kJ/M^2 , which is somewhat higher than that estimated from the single-specimen J-integral values. However, given the significant differences in both analysis and test details between these two methods, the authors consider this to be a reasonable agreement between these methods. Other researchers have argued the equivalence of these two methods from analytical viewpoints,⁹ including constitutive effects for elastomeric materials, which were not considered here. Because both methods produce similar results for the critical fracture energy, additional tests utilized the J-integral single specimen test method because less material is required.

Effect of Specimen Geometry

Another series of experiments were conducted to evaluate the invariance of the fracture energy on specimen geometry. Again, the TPE6114 elastomer formulation was used for this comparison. For this study, a second set of J-integral fracture studies were conducted on a double edge-notched test specimen. Results from the double edge-notched specimen produce a fracture energy of 48 kJ/M^2 , which is essentially the same for the center-notched specimens. This further supports the view that the single-specimen J-integral approach can be used, and that either center- or double edge-notched specimens can be used.

Effect of Material Composition on Fracture

To study the effects of elastomer composition on the fracture energy, the authors adopted the center notched geometry, and have compared the critical J-integral value of the three TPEs (see Table II). The major factor affecting fracture toughness appears to be the weight percentage of the three blend components. TPE6101 consists of 40% elastomer, compared with 25% for TPE6114,

Table II Comparison of the Fracture Behavior of the Elastomers Investigated Herein

Formulation	J_{1C} (kJ/m^2)	Slope of " $J-\Delta a$ " Curve (MJ/m^3)
TPE6114	46	5.8
TPE6112	42	5.2
TPE6101	24	1.6

Results were obtained from J-integral tests on center-notched samples.

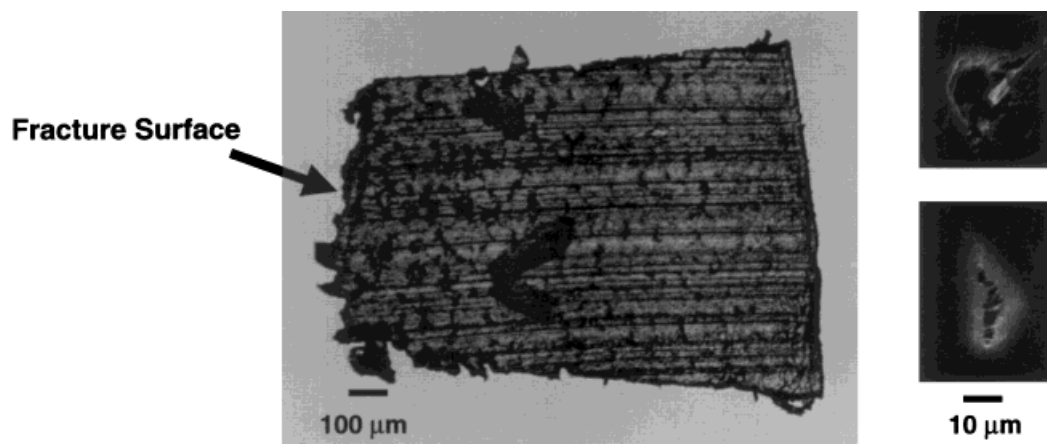


Figure 3 Combined TOM micrograph and SEM micrographs of the process zone associated with crack growth of the J-integral test for TPE6114. The crack growth direction is perpendicularly out of the page, and the fracture surface is indicated. The flaws that make up the process zone are both voids and crazes (see inserts). The dimensions of these flaws are generally between 10 and 30 μm .

and subsequently has a markedly reduced resistance to fracture in terms of both the critical J-integral value (24 kJ/m^2 compared with 46 kJ/m^2) and in slope of the J-integral vs. crack extension graph (1.6 MJ/m^3 compared with 5.8 MJ/m^3). The former represents the resistance to crack initiation, and the latter, the resistance to crack growth. It is unclear whether this is due to high elastomer content blends being innately weak or whether this is due to the large amount of processing oil required to process high elastomer content blends. By comparing the fracture of TPE6112 and TPE6114, it is apparent that changing the molecular weight of the iPP had only a marginal affect on the fracture properties. Both the critical J-integral value and the slope of the J-integral vs. crack extension graph are slightly reduced by implementing a more viscous (higher molecular weight) grade of iPP.

Micromechanisms of Fracture

The previous section showed that the fracture energy and stability are highly dependent on the composition and morphology of the EPTPE blend. Different compositions damage to different extents as the composition is altered. It is well established that the damage that proceeds and surrounds the crack consumes a significant amount of the fracture energy, and often accounts for a major part of the material's resistance to fracture. Consequently, it is useful to identify the micromechanisms associated with the fracture process

to help guide development of these materials. The following discussion of the morphological changes resulting from fracture and micromechanisms of fracture is based solely on results observed in TPE6114.

During the fracture tests, a process zone of damage was observed in the optical stereomicroscope by the scattering of white light transmitted through the sample. To isolate the micromechanisms associated with this damage, optical sections were cut perpendicular to the fracture surface through the damaged material. These sections were cryo cut using liquid nitrogen cooling and a glass knife; they could then be examined by transmission optical microscopy (TOM). Similarly oriented block faces were microtomed smooth in a liquid nitrogen cooled microtome, and then coated in gold and examined using scanning electron microscopy (SEM).

Figure 3 shows a composite of TOM and SEM micrographs from a section cut through the damage area of a J-integral test sample (note that the fracture surface is on the far left). The whitening macroscopically visible is evident here as a series of vertical dark streaks perpendicular to the stress direction. The horizontal streaks are microtome knife marks and the V-shape in the lower half of the image is a second smaller section—both should be ignored. Closer inspection of the damage features by SEM showed that these defects are, in fact, both crazes and voids (see inserts on right). The size of these flaws varies from

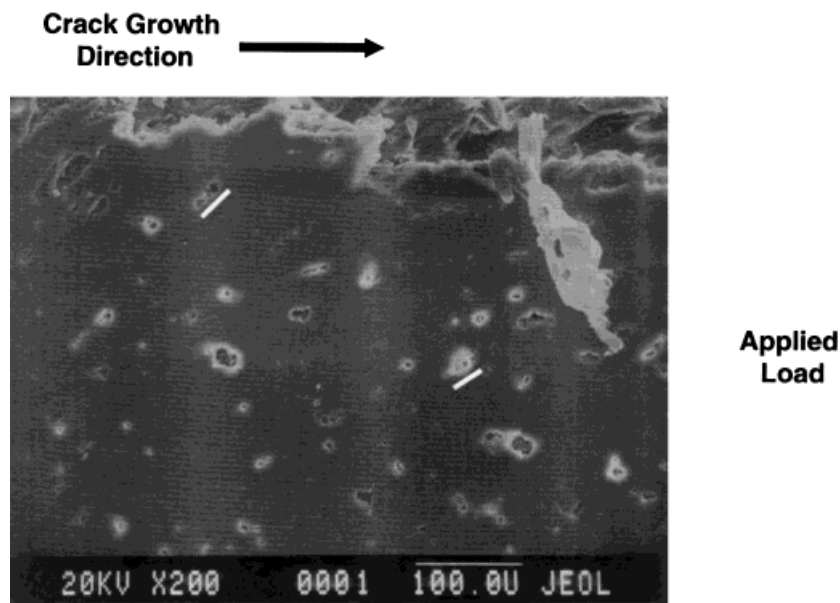


Figure 4 SEM micrograph of the process associated with crack growth in a J-integral test on the TPE6114 samples. The crack growth direction is from left to right, and the fracture surface is indicated at the top of the image. As in Figure 3, the process zone flaws can be seen to be both voids and crazes. However, from this orientation it can be seen that many of the crazes are aligned obliquely to the overall crack growth direction, and that the texture of the fracture surface is parallel to these oblique crazes. Two oblique crazes have been highlighted.

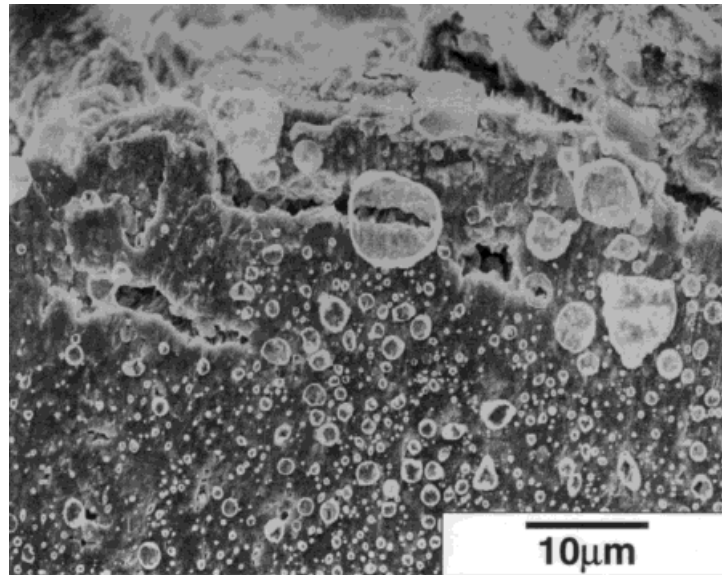
10 up to 30 μm . Note that these flaws are larger than the discrete elastomer domain size ($1\text{--}3\ \mu\text{m}$)⁴ within the continuous polypropylene matrix by an order of magnitude. From these sections the crazes appeared to be, in general, perpendicular to the applied load direction, although the shape of the crazes is often tortuous. It is evident from Figure 3 that the density of crazes is greatest near the fracture surface and gradually decreases with increasing distance from the fracture surface. This is in accord with the diffuse nature of the damage zone in Mode I fracture tests.

Further information can be gathered from examination of damage in sections cut parallel to both the crack growth direction and the direction of applied load (see Fig. 4). Again, both voids and crazes are observed, but in these sections the crazes are seen to grow obliquely to both the applied load and the crack growth direction. The orientation of these oblique crazes to the direction of crack growth clearly indicates that these oblique crazes are not shear bands. It is known that at the crack tip the stress state is triaxial, and hence, it is not surprising that the stress direction in the proximity of the crack tip is oblique to the applied load. This local stress state

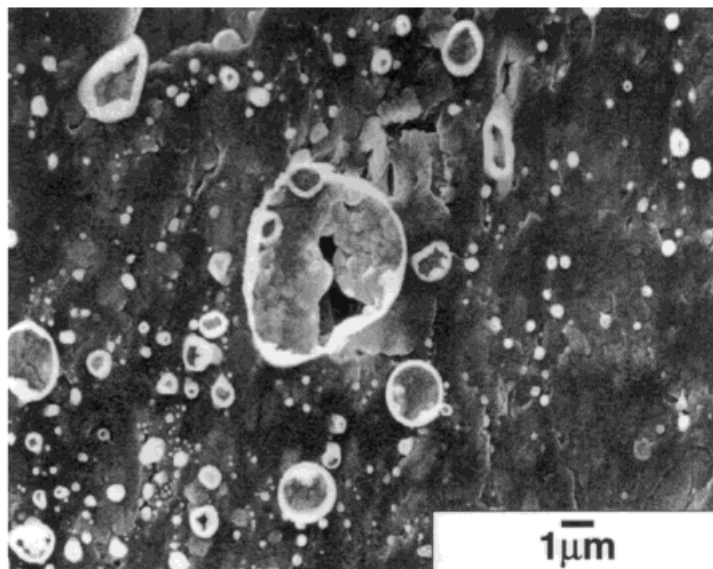
could account for these crazes being oriented obliquely to the overall crack growth direction. These oblique crazes could account for the nature of the highly textured fracture surface (see the top of Fig. 4).

Microscopic examination of the process zone associated with crack growth in the essential work samples reveals a similar scheme of damage. The process zone consists of an array of voids and crazes that are an order of magnitude larger than elastomer phase domains. The crazes are aligned obliquely to the overall direction of the crack growth, and there is a highly textured fracture surface, possibly due to the oblique crazes.

A block face cut from within the process zone, perpendicular to the crack growth direction, was cryo-microtomed, stained using ruthenium vapor, and then examined using SEM (see Fig. 5). The ruthenium preferentially stains the elastomer-rich regions; these become electron dense, emit more secondary electrons, and hence, appear as the bright domains in Figure 5. Figure 5(a) shows many interesting features of the damage mechanisms in these polymer systems. For the crazes and voids to be many times the size of the discrete elastomer domains it is necessary that these



(a)



(b)

Figure 5 SEM micrographs of a cryomicrotomed and then ruthenium stained block face of the process zone around crack growth in TPE6114. The loading direction is vertical and the overall crack growth direction is out of the page. (A) Shows details of a crack growing through both polymer and elastomer domains (top–middle) and a craze in which at least one fibril consists of elastomeric material. (B) Illustrates a voided elastomer-rich domain.

crazes and voids exist within the polypropylene domain and possibly the elastomer domains as well. In the top middle of Figure 5(a) there is an example of a craze that has passed through both the polypropylene domain and an unusually large (8 μm) elastomer domain. It is apparent that the

material between the craze faces within this elastomeric domain is highly fibrillated. Furthermore, the craze at the middle left of Figure 5(a) has grown through the lower part of an elastomer domain, and an elastomeric fibril has extended between the two faces of the craze. The elastomer

domain shown in Figure 5(b) has become voided in a manner reminiscent of that in many other elastomer toughened polymeric systems.

CONCLUSIONS

The fracture behavior of three model EPTPEs illustrates that these are tough materials. For the model EPTPE KW6114, we confirm that measurements of critical energy release rate (46 kJ/m^2) and essential work (54 kJ/m^2) are equivalent. Furthermore, changes to the sample geometry were not found to affect the critical energy release rate (double edged notched, 48 kJ/m^2 , and center notched, 46 kJ/m^2). Increasing both the elastomer and processing oil components of these blends was found to drastically reduce the resistance to fracture initiation and propagation. Increasing the molecular weight of the thermoplastic phase was found to marginally reduce the material's resistance to fracture initiation and propagation. Moreover, these materials fracture in a stable fashion, and no evidence of instability was found.

The micromechanisms of damage occur as an array of crazes and voids, which increase in density as the fracture surface is approached. Further, these flaws are of a scale that is approximately one order of magnitude larger than the

heterogeneous texture of the alloy (i.e., the domain size of the elastomer phase). It was found that these flaws grow through both the polymer and elastomer domains, and that at least some of the craze fibrils consist of the elastomer phase.

The authors gratefully acknowledge Advanced Elastomer Systems and Exxon Chemical Company for their financial support and materials provided for this study. Also, the authors would like to thank Dr. M. D. Ellul for her many thoughtful comments and suggestions throughout this study.

REFERENCES

1. Ellul, M. D.; Hazelton, D. R. *Rubber Chem Technol* 1994, 67, 582.
2. Ellul, M. D.; Patel, J.; Tinker, A. J. *Rubber Chem Technol* 1995, 68, 573.
3. Rivlin, R. S.; Thomas, A. G. *J Polym Sci* 1953, 10, 291.
4. Thomas, A. G. *J Appl Polym Sci* 1960, 3, 168.
5. Rice, J. R. *J Appl Mech ASME* 1968, 35, 379.
6. 1988 Annual Book of ASTM Standards, 03.01, 698 (1988).
7. Broberg, K. B. *Int J Fract* 1968, 4, 11.
8. Paton, C. A.; Hashemi, S. *J Mater Sci* 1992, 27, 2279.
9. Mai, Y. W.; Powell, P. *J Polym Sci Part B Polym Phys Ed* 1991, 29, 785.